CHAPTER 49

DECOMPOSITION OF CO-EXISTING RANDOM WAVE ENERGY

Dennis B. Morden[1], Eugene P. Richey[2] and Derald R. Christensen[3]

INTRODUCTION

Of the several transformations that water waves may undergo, the phenomenon of reflection has received relatively little quantitative attention, although the analyst is sensitized to reflection in a qualitative way. Commonly the investigator is interested in progressive or transmitted waves and the characteristics of reflected waves and the energy dissipated during the reflection process are of little consequence. There are, however, certain structures, such as piers, floating bridges, bulkheads, etc., where waves reflecting from the structure can be of concern if they should impinge on a site or shoreline sensitive to a new, or changed, wave climate. Quantitative assessment of the energy dissipated during reflection is essential to the evaluation of devices which are intended to reduce site interaction problems and/or reduce the loading on structures and anchor systems.

This paper examines the analysis of sea states where wind-generated waves and their reflection co-exist. Using the results of a field test the characteristics of co-existing sea states are discussed. The decomposition of these waves to obtain separate incident and reflected wave spectra requires two applications of spectral analysis. First, spectral estimates are computed from co-existing wave data acquired simultaneously at multiple, fixed sensor locations. These spectra are then divided into frequency increments and the amplitude associated with each increment used as an independent input into a technique to decompose the co-existing waves into appropriate incident and reflected wave spectra. Because the incremental amplitudes of the original spectral estimates are used as independent inputs, the shape and accuracy of these original estimates naturally have a profound influence on the final separated wave spectra. Various spectral estimating techniques were used on the field data and the accuracy of the results were compared to three validation criteria.

Because the findings and discussion are validated primarily by the analysis of specific data it seems appropriate to first describe the relevant features of the field test. Though the present study involves deep water waves and zero transmission, the principles apply equally well to any situation where wave reflections are of interest.

TEST DESCRIPTION

Test Site - Sea states composed of wind-generated deep water waves and their reflections were examined in Lake Washington which adjoins Seattle,

1. Research Engineer, The Boeing Company, Seattle, Washington, U.S.A.
2. Professor of Civil Engineering, Department of Civil Engineering, University of Washington, Seattle, Washington, U.S.A.
3. Research Engineer, Department of Civil Engineering, University of Washington, Seattle, Washington, U.S.A.

Washington, U.S.A. A sixty-foot wide floating bridge with a seven-foot draft traverses the lake in a generally east-west direction and is exposed to waves generated over a 2.8 mile effective fetch by the prevailing southerly winds of the region. Near the center of the span a test site was established to evaluate the waves reflected from the solid vertical walls of the bridge pontoons (which extended 11 feet above SWL) and those reflected from a perforated wall breakwater appended to the pontoon. For the waves occuring at the site the bridge forms an excellent barrier, completely eliminating transmitted waves. The 200-foot depth of the lake is sufficient to classify all waves as deep water waves. During storms reflected wave trains are apparent as far as 4,000 feet south of the bridge.

Figure 1 depicts an aerial close-up of the test site. Co-existing incident and reflected waves were monitored using pressure transducers located five feet below stillwater level (SWL). Analog data were recorded simultaneously at four locations: two in front of a breakwater and two more 150 feet away in front of the solid vertical wall of the bridge. Viatran Model PTB 101 transducers were rigidly mounted 7'9" and 12'9" away from each barrier, as shown in the figure. Morden (1975) shows details of the apparatus and test procedure.

Perforated Wall Breakwater - To produce reflected waves with amplitudes substantially different from those at the solid vertical bridge wall, a perforated vertical wall and solid (but removable) bottom were appended to the bridge, as shown in Figure 2. This "L"-shaped structure and resulting chamber form a perforated wall breakwater of the type originated by Jarlan (1961). The test breakwater section was long enough to avoid diffraction effects on the outer wave sensors, and terminated by solid vertical end plates to maximize the two-dimensional response of the chamber.

Several authors have tested and analyzed the behavior of this type of breakwater; their results have been reviewed by Morden (1975). Richey and Sollitt (1970) successfully model the behavior of the breakwater in monochromatic waves as a linear damped oscillator. As such the amplitude and phase angle of a wave are altered during the reflection process, but its frequency is not changed.

The reflection coefficient for the breakwater in monochromatic waves (Fig.3) is defined as the ratio of reflected to incident wave heights, and has a minimum value at a particular frequency, which depends primarily upon breakwater geometry. This definition must be modified for the random wave case, and becomes the square root of the ratio of the reflected to incident energy over a specified frequency band width, i.e.,

$$R = \sqrt{\frac{\sigma_r^2}{\sigma_i^2}} \qquad (1)$$

CHARACTERISTICS OF CO-EXISTING* SEA STATES

Ippen (1966, p. 58) points out that the average potential energy density (i.e., potential energy per unit surface area) is a function of distance from

* Sea states composed of the superposition of wind-generated waves and their reflections. Superposition of unrelated waves are not considered.

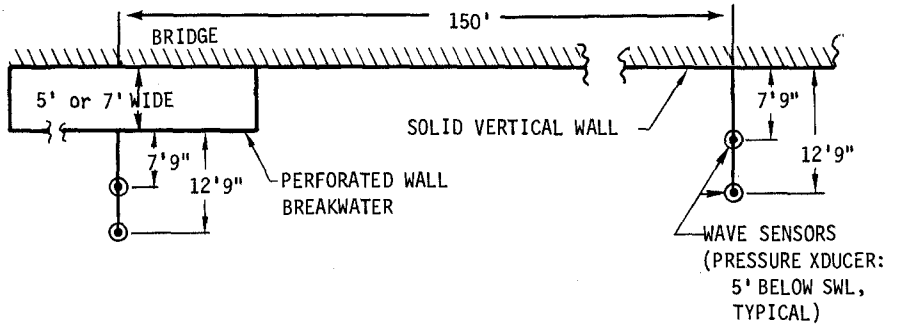

FIGURE 1: AERIAL SCHEMATIC OF TEST SITE SHOWING WAVE SENSOR LOCATIONS

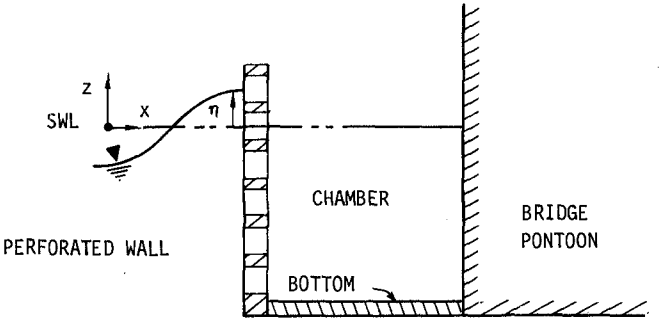

FIGURE 2: CROSS SECTION OF PERFORATED WALL BREAKWATER

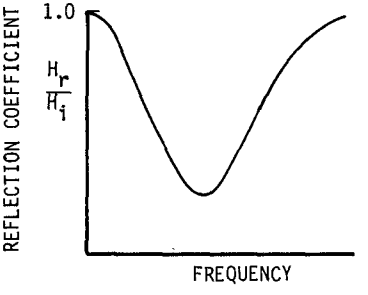

FIGURE 3: TYPICAL PERFORMANCE OF PERFORATED WALL BREAKWATERS

the reflecting barrier. For a single linear wave component the time averaged potential energy at a fixed location, x, obtained from the application of linear wave theory is

$$PE(x) = \frac{\gamma}{4}\left(a_i^2 + a_r^2 - 2\, a_i a_r \cos\left(\theta_r + \frac{4\pi x}{L}\right)\right) \qquad (2)$$

where a_i, a_r, L, and θ_r are the incident and reflected wave amplitudes, wave length, and relative phase angle, respectively. Since the wave sensors monitor the potential energy, the time averaged energy density at a fixed location in a co-existing sea state is not the same as the sum of the time averaged energy densities (taken independently) of the incident and reflected progressive waves that combine to form the co-existing waves. The measured amplitude is modulated by the last term of Eq. 2.

Inherent in the computation of average energy density for a progressive wave is the assumption that the time average of the wave amplitude at a fixed location is the same as the spatial average of the wave amplitude at a fixed time. For random progressive waves this requirement is met statistically by assuming that the random process is ergodic; i.e., that the ensemble average equals the time average for any location and time. Random waves progressing in a given direction are represented as the superposition of a number of components each with its own characteristic amplitude, frequency, speed, length, and phase angle. The phase angles for random progressive waves are taken to be independent, random, and uniformly distributed between 0 and 2π. When a random progressive wave and its reflection co-exist there is a deterministic relationship between each incident and reflected wave component. The relationship is a function of the speed of the wave component, the distance between the sensor and the location of reflection, and the phase change occuring during the reflection process, if any. The speed associated with each component is linearly related to the frequency such that product of the frequency and speed is a constant.

Any two components of a progressive wave move into and out of phase with each other as time progresses, causing a beat effect. If energy density for progressive waves is averaged over a beat period, the average energy density is <u>not</u> a function of location and the average value equals the sum of the energy densities for each component.

On the other hand, the time series obtained at a fixed location in a co-existing incident-reflected sea state not only contains the beat effect for each wave system but also the amplitude modulation which is a consequence of being, in effect, at different locations on a partial standing wave envelope for each frequency component. For each frequency component the amplitude modulation has a different value (due to the space and frequency dependence of the last term in Eq. 2). The net result is a time series with a beat effect and an amplitude modulation causing the peak measured amplitude values to be strongly dependent on sensor location. The effects are evident in the typical time series shown in Figure 4 for data acquired simultaneously at two fixed locations in front of a solid vertical wall. The effect of position in a standing wave envelope is evidenced by the maximum values recorded. Signals obtained in front of the breakwater are similar in appearance.

Spectra obtained from these time series are shown in Figure 5. The

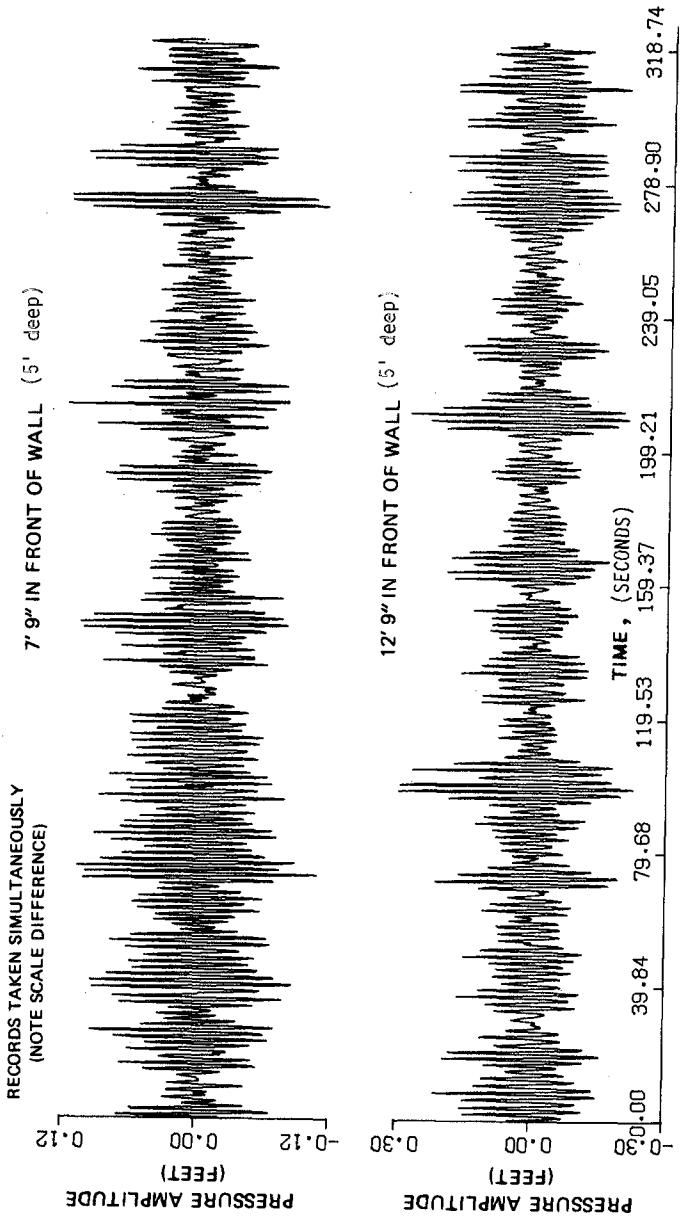

FIGURE 4: TYPICAL TIME SERIES AT TWO LOCATIONS IN FRONT OF A SOLID VERTICAL WALL.

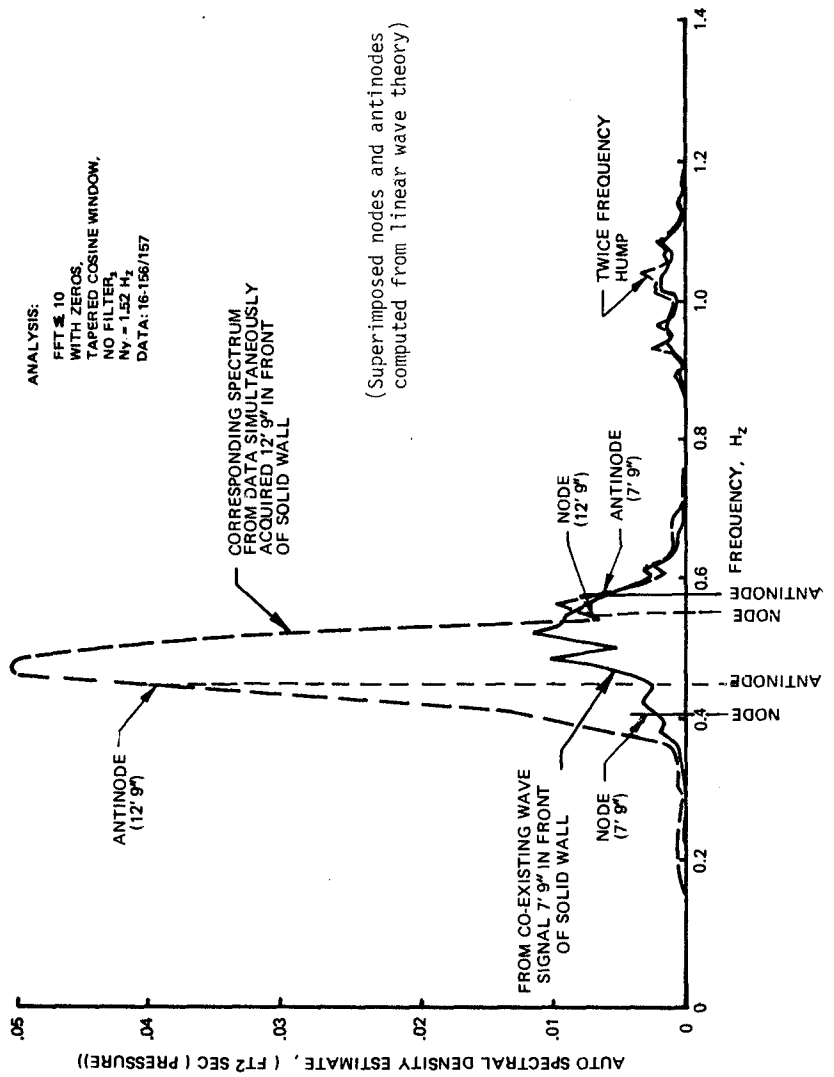

FIGURE 5: CO-EXISTING WAVE SPECTRA FROM PRESSURE DATA IN FRONT OF SOLID VERTICAL WALL.

variances computed at the two distances in front of the solid wall display a strong dependence on sensor location. The twice frequency hump is due to using subsurface pressure sensors. Longuet-Higgins (1950) and Silvester (1974) established that in co-existing sea states a second order pressure variation of the form $\frac{\gamma\pi a_i a_r}{L}\cos(4\pi ft)$ exists in addition to the usual. The term is not attenuated with depth and ultimately dominates over the first order term (with its $e^{2\pi z/L}$ pressure response factor) as depth increases. The second order term can be attributed to the movement of the center of gravity in the water column as above the sensors, the fluctuations, occuring at twice the frequency of the surface wave components, are not "real" in the sense of contributing to the surface energy density and therefore must be filtered from spectra obtained using pressure sensors in co-existing sea states.* In the present study the filtering was not a problem, but in co-existing sea states where the spectrum is relatively broad band (the twice-frequency hump might be buried in the spectrum) surface piercing gauges should be used.

The characteristics of the remaining spectra may be better understood by considering a single frequency component of both the incident and reflected wave system. Conceptually, the resulting sea surface at a fixed location due to these two components can be thought of as the sum of a progressive wave and a standing wave. The progressive component eliminates the possibility of true nodes, while the standing wave component produces maxima and minima in the wave envelope which are functions of location. Since these locations are determined by the standing wave component, the phase angle and distance relationships producing the amplitude extremes can be obtained by examining the nodes and antinodes for a perfect reflection. The frequencies associated with node and antinode locations for perfect reflection were computed from linear theory and superimposed on Figure 5. The nodes and antinodes suggest frequencies at which the spectra for each fixed location should contain minimum and maximum (respectively) amounts of information about the wave process. When simultaneously acquired co-existing wave data are examined at two fixed locations, the effects of spatial dependence of the information contained in the spectra can be seen. No location exists where the computed spectrum contains the appropriate ordinate values for the process at all frequencies. Instead, the location where the largest variance (and spectral area) will be calculated is at the position where the frequency for an antinode most nearly matches the peak frequency of the incident wave (assuming that the band width of the process is on the order of, or less than, the frequency difference between nodes). For the wind condition represented by Figure 5, the majority of the incident wave energy occurs at frequencies (.4 - .5 HZ) near a node at the inner (7'9") station and near an antinode for the outer (12'9") station. The opposite occurs in the high frequency tail of the curves where the spectral ordinate value associated with the outer station is less at a frequency corresponding to a node. Since the energy in the incident wave was concentrated

---

* Alternative one could analyse only the twice frequency spectrum because it is not attenuated with depth, provided the size of the $\frac{\gamma\pi}{L}a_i a_r$ terms are sufficient to analyse. Due to the considerable reduction in a_r caused by the breakwater the twice frequency hump was exceedingly small for spectra obtained from data taken in front of the breakwater.

in a frequency range near the antinode for the outer station, its calculated variance is much larger than that for the inner one (in this case 4.6 times as large). For all wave conditions tested, the peak incident wave frequency was nearer the antinode frequency for the outer station. Thus, the variance calculated at that station was always larger than the variance at the inner one. The ratio of the variance at the two stations (outer/inner) ranged from 1.4 to 8.1 for the wave conditions of record.

When a linear reflection process occurs at barriers other than solid vertical walls, the location of the node and antinode associated with each frequency increment is altered due to the phase changed occuring during the reflection process. As a result of the phase change during reflection altering the frequencies associated with nodes and antinodes, a fixed location in front of the breakwater is not monitoring the same portion of the partial standing wave envelope as that being monitored at the same physical distance in front of a solid vertical wall. Thus, direct comparison of spectral ordinate values obtained from co-existing wave data taken at the same physical distance in front of two types of barriers is a comparison of "apples and oranges."

Having discussed the behavior of co-existing sea states and demonstrated that the variance obtained from any fixed sensor data does not represent the true average energy density, a technique is now discussed to circumvent the problems and decompose multiple co-existing wave spectra into separate incident and reflected spectra.

DECOMPOSITION TECHNIQUE

Thornton and Calhoun (1972) initially presented a theory for separating incident and reflected wave spectra using co-existing wave data acquired simultaneously at two fixed locations in line along the wave ray. The sea state is presumed to result from the superposition of random waves progressing in opposite directions. Each wave is assumed to pass over both sensors. As commonly done in spectral analysis, the random waves progressing in a given direction are represented as the superposition of a number of components each with its own characteristic amplitude, frequency, speed, length, and phase angle. The phase angles for random progressive waves are taken to be independent, random, and uniformly distributed between 0 and 2π. Spectral analysis is used to compute mean square spectra (as well as cross spectra) for the co-existing waves at each sensor location.

The theory was developed by applying linear wave theory to mono-chromatic waves. For a single wave component frequency, the incident and reflected component wave amplitudes are related to the co-existing wave amplitude at two stations. The resulting equations are:

$$\theta_r = \tan^{-1}\left[\frac{A_1 \cos kx_2 - A_2 \cos \theta}{A_1 \sin kx_2 - A_2 \sin \theta}\right] \qquad (3)$$

$$\theta_i = \tan^{-1}\left[\frac{a_r \sin \theta_r}{A_1 - a_r \cos \theta_r}\right]$$

$$\theta_i = \tan^{-1}\left[\frac{A_1 \cos kx_2 - A_2 \cos \theta}{A_1 \sin kx_2 + A_2 \sin \theta}\right] \quad (4)$$

$$a_r = \frac{-A_2 \cos \theta + A_1 \cos kx_2}{2 \sin kx_2 \sin \theta_r} \quad (5)$$

$$a_i = \frac{a_r \sin \theta_r}{\sin \theta_i} = \frac{A_1 \cos kx_2 - A_2 \cos \theta}{2 \sin kx_2 \sin \theta_i} \quad (6)$$

The quantities A_1 and A_2 are the amplitudes of the particular frequency component under consideration as calculated from spectral analysis of the signals at 1 and 2. x_2 is the measured distance between gauges; k is calculated from linear wave theory to be $k = 2\pi/L = (4\pi^2/g)f^2$ (in deep water). The phase relationship θ can be obtained directly from the data through cross-spectral analysis of simultaneously acquired records at the two in-line sensor locations. The cross-spectrum is obtained from the Fourier transform of the cross-covariance function in the same manner that the energy spectrum is obtained from the Fourier transform of the auto-covariance function. The inverse tangent of the odd contribution to the cross-spectrum (quadrature spectrum, $Q_{12}(f)$) divided by the even contribution (co-spectrum, $C_{12}(f)$) can be used to calculate the average phase shift, θ, within each frequency band; i.e.,

$$\theta(f) = \tan^{-1}\left[\frac{Q_{12}(f)}{C_{12}(f)}\right] \quad (7)$$

These quantities are sufficient to solve for θ_r and θ_i using Equations 3 and 4. The values of a_r and a_i are then available as a function of these phase angles for the given frequency.

Thus, by evaluating each frequency bandwidth using Equations 3 - 7 the component incident and reflected wave amplitudes can be calculated and the corresponding separate incident and reflected wave spectra computed. In random waves, A_1 and A_2 are obtained by applying spectral analysis to the measured co-existing wave data. The resulting co-existing wave spectra are necessarily only estimates of the distribution of amplitudes (squared) with frequency (i.e., each co-existing wave spectrum is divided into frequency increments and the amplitude representative of that frequency band used as an independent input to equations 3 - 7.). Incident and reflected spectra are then created by plotting the solution to the equations (at each frequency increment) over the range of frequencies. Thus, the accuracy of the resulting spectra is strongly dependent on the shape as well as the variance of the co-existing wave spectra. The process is reviewed schematically in Figure 6. The assumptions inherent in the application of the technique include:

1. Linear wave theory applies. This requirement, which is a reasonable engineering approximation for most non-breaking sea states, is due to the linear wave theory applied to solve the equations.

2. The reflection process does not alter the frequency. Since each

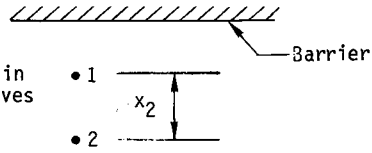

DATA: From multiple fixed sensors in co-existing waves

SPECTRAL ESTIMATES OF CO-EXISTING WAVE SIGNALS:

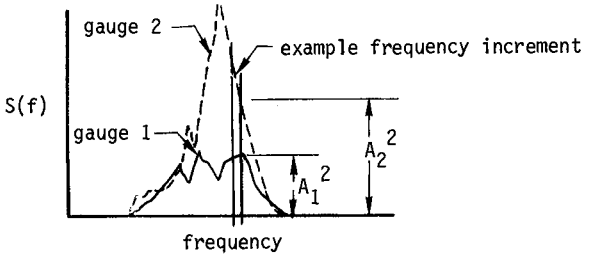

DECOMPOSITION:

- Divide co-existing spectrum into frequency increments
- Apply linear wave theory to each frequency increment independently
- 4 equations f(A_1,A_2,x_2,relative phase)
- Solve for incident and reflected wave amplitude and phase

OUTPUT:

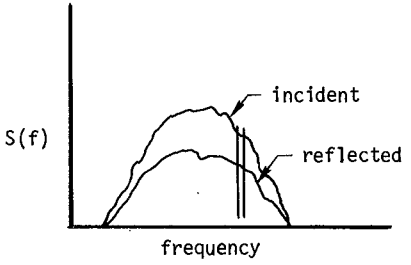

- If accurately computed, σ_i^2 and σ_r^2 are independent estimates and can be used directly to evaluate reflection coefficients and energy dissipation

FIGURE 6: OUTLINE OF DECOMPOSITION TECHNIQUE

frequency increment is treated independently there is no analytical mechanism to account for frequency alterations.

3. Wave crests are sufficiently long and parallel to the reflecting barrier that the incident wave passes both sensors, is reflected and passes both sensors again.

4. The surface at each sensor location is the linear superposition of progressive incident and reflected waves.

5. The process is statistically stationery. Typically this requirement is met by comparing calculations based on different portions of an analogue data record.

The distance between sensors must be known, but it is not necessary to know the distance to the reflecting barrier nor the characteristics of the reflection process (except for requirement #2 above).

To evaluate the accuracy of various spectral analysis techniques three performance criteria were specified for the test data. Before the particular techniques are compared, some general characteristics of the spectra resulting from decomposing the co-existing waves are presented.

The required inputs for the decomposition technique are the incremental amplitude and phase information obtained from spectral estimates of two simultaneously acquired co-existing wave signals taken at two different distances in front of a reflecting barrier. The incident waves must have crests nearly parallel to the reflection barrier and the sensors sufficiently in-line with the wave advance that any given incident wave component can be assumed to pass both gages, be reflected, and again pass both gages.. Linear wave theory is then used to separate the incident and reflected components from the co-existing wave components at the two fixed locations on the partial standing wave envelope. Because each frequency increment is treated independently, it is necessary to know or assume that the reflection process does not appreciably alter the frequency of the incident wave component. It is not necessary to know anything else about the location or characteristics of the reflection process.

The technique produces the phase and amplitude for both the incident and reflected spectra at each frequency increment. These are presented in Eqs. 2 - 6 and are functions only of the physical distance between sensors and the characteristics of the co-existing wave signals.

Surface or subsurface wave sensors can be used to obtain the co-existing wave information. If subsurface transducers are used the twice frequency components must be filtered from the spectra before they are input to the decomposition technique.

Eqs. 3 - 6 are consistent if the outer gage is designated 1 and inner gage 2. The two signals can be interchanged if the sign on the phase angle, θ, is changed. Usually, an auto spectrum can be calculated without regard to the sign of the amplitude. Due to the use of information from two auto spectra in calculating the incident and/or reflected spectra using this technique, the

signs must be consistent with the physical signal (or both opposite from reality).

Figure 7 shows the reflected wave spectrum in front of a solid vertical wall (from the co-existing wave spectra shown in Figure 5). From Figure 5 it can be seen that the amplitude values at frequencies below .2 Hz are extremely small. Terms involving the difference of these small values are used in the denominator of the equation for amplitude (Eq. 5). Thus, the values of the reflected spectra calculated where the amplitudes of both co-existing spectra are nearly zero ($f<.2$) is erroneous and should be set to zero.

The denominator of Eq. 5 goes to zero when the wave length equals twice the spacing between the sensors. For the distance between the sensors in the present investigation of five feet the amplitude should go to infinity at $f = .716$ Hz. This is clearly evident on Figure 7. For any application of the technique the distance, x_2, between the sensors should be chosen so that $\sqrt{x_2/2.56}$ is greater than any frequency containing surface wave data of interest.*

The remaining spectral information, which for the figure shown is concentrated between $f = .35$ and .65 Hz., is the actual spectral estimate associated with the reflected wave that contributed to the co-existing sea state of Figure 5. Due to the equation similarity, the incident spectrum has identical characteristics.

Eqs. 4 and 6 are written in two forms which are trignometrically identical. The numerical problems discussed relative to frequencies below .2 Hz produce different spectral calculations for the different identities below $f = .2$ Hz and above $f = .75$ Hz (because the input amplitudes were nearly zero). Over the range of interest, i.e., the range of frequencies when the co-existing wave spectra indicated wave activity, the identities produced identical answers.

For any application of this technique, the range of frequencies containing surface wave information should be established from the co-existing wave spectra and/or knowledge of the specific test conditions. Outside the desired range the extraneous incident and reflected spectral amplitude should be filtered off. The variances of the resulting incident and reflected spectra can then be obtained.

These variances now represent the average energy densities in the incident and reflected wave process and are independent. Since they are separate from each other and independent of spatial location, they can now be used directly to calculate the reflection coefficient of a barrier and/or the dissipation occurring during reflection. The dissipation is easily expressed as the decrease in average incident energy ($\propto$ incident variance, σ_i^2, and reflected variance, σ_r^2).

$$\text{Percent dissipation during reflection} = \left(1 - \frac{\sigma_r^2}{\sigma_i^2}\right) \cdot 100 \qquad (8)$$

---

* From linear deepwater wave theory, $f = \sqrt{\frac{5.12}{L}}$. The decomposition is valid for wave lengths greater than $2x_2$.. '. decomposition is valid for $f<\sqrt{x_2/2.56}$.

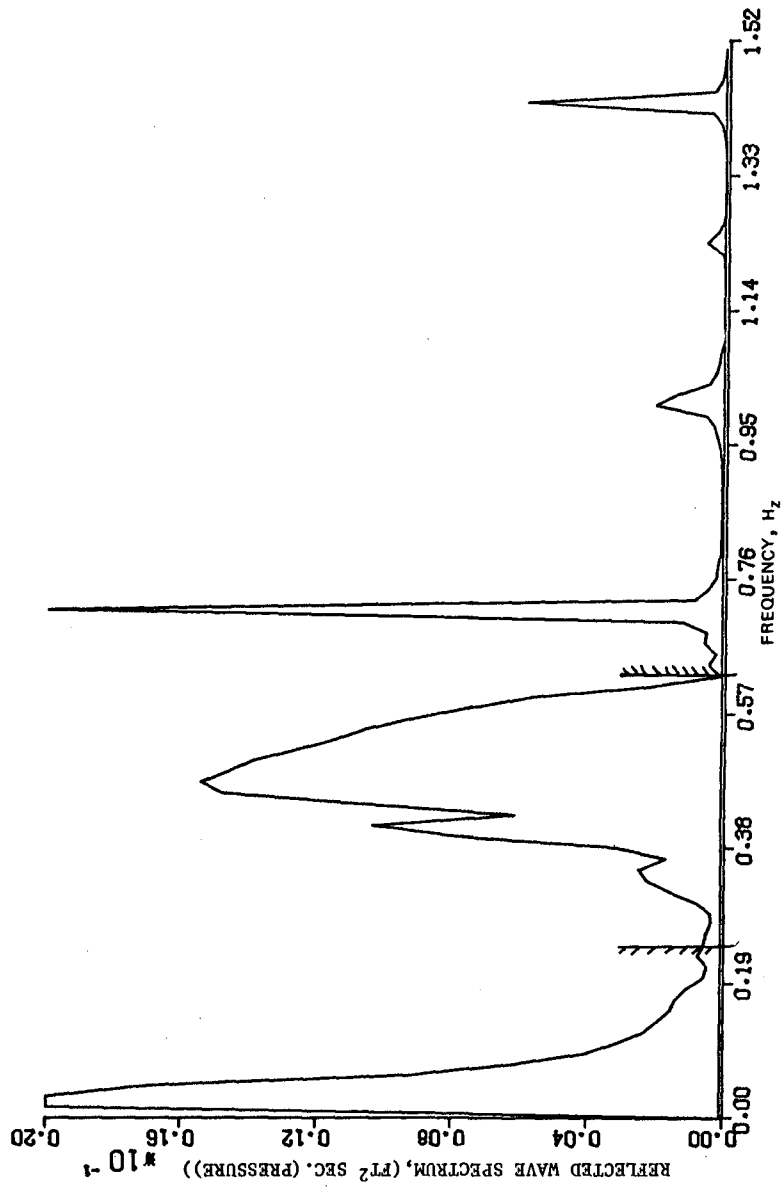

FIGURE 7: AUTO-SPECTRUM FOR REFLECTED WAVE IN FRONT OF SOLID WALL; COMPUTED BY DECOMPOSITION OF CO-EXISTING WAVES.

Either the reflection coefficients or the dissipation can be calculated equally well from the surface or sub-surface sensor data once the desired frequency range has been defined (and provided the pressure response factor does not reduce the signal strength to an unacceptable level within the range of interest).

A technique has thus been shown to circumvent the problems associated with co-existing random wave data, and produces separate incident and reflected spectra from which the desired reflection characteristics of a barrier can be obtained. The only requirements to using the technique are (1) that the reflection process be known or assumed to occur without altering the wave component frequency, (2) that the distance between two in-line sensors be known, and (3) that the co-existing wave spectra from the two sensors be used as inputs to the decomposition technique where each frequency increment of the spectra is operated on independently. The effect of the last requirement on the numerical computation of incident and reflected spectra is now considered.

COMPARISON OF LAG PRODUCT AND FAST FOURIER TRANSFORM METHDDS APPLIED TO THE DECOMPOSITION TECHNIQUE

The decomposition technique requires, as input information, the auto and cross spectra from data acquired simultaneously at two "in-line" locations in a sea state where random incident waves and their reflections co-exist. Increments of the auto spectra become the inputs to Eqs. 3 - 6 and increments of the cross spectra are used to evaluate the phase, Eq. 7. The technique operates on each frequency increment of the spectra independently. Thus the shape and accuracy of the co-existing wave spectral estimates could profoundly influence the computed incident and reflected spectra.

Two methods are commonly used to obtain spectra from random signals; namely, lag product and fast Fourier transform techniques. The lag product method follows the procedure given by Jenkins and Watts (1968). A fast Fourier transform program is described by Paniker (1971). Programmed versions of both methods are widely available. The lag product method involves computing the autocovariance function, which is the correlation of the random signal with itself for the desired number of lags (time increments). The zero lag product of the process is the variance, or mean square value of the signal about the mean. The mean is always zero for the present investigation and the variance is directly proportional to the average energy in the wave signal, and the Fourier transform of the autocovariance function is the spectrum.

Parseval's Theorem (Brigham, 1974) establishes that the spectrum also results from the direct Fourier transform of the continuous time series. For digital computation the Discrete Fourier Transform, DFT, provides a Fourier transform pair made up of the digital time series and a discrete approximation of the continuous spectrum. The fast Fourier transform, FFT, is just an algorithm for efficiently computing the DFT (Bergland, 1969).*

---

* For 1024 data points used for most of the present analysis the FFT produces a 2DD to 1 reduction in computation relative to the DFT.

The transformations above are defined for infinite time. For the finite length records actually used the transformation can be thought of as an infinite time series multiplied by a window with length equal to the data record. Since multiplication in the time domain is convolution in the frequency domain, the transform of the data (or autocovariance function) is automatically convolved with the transform of the window function. When no window shape is specified it automatically becomes a function which equals zero for all time except the time of the data record and equals one (i.e., has no effect on the time series) during the time of the record (referred to as a rectangular window). The transform of the rectangular window has substantial side loops, which when convolved with the transform of the data produces undesirable positive and negative contributions to the spectral value at each frequency. To minimize this effect several window functions are in common usage which, when transformed, have smaller or better behaved side loops and produce more desirable or less noticeable contributions to the spectral estimate. Though the effect of convolving the data with a window can be reduced through the choice of window functions, the resulting spectrum is always an estimate of the true spectrum for the process.

The spectrum resulting from the transformation of the finite digitized data is referred to as a raw periodogram. Since the periodogram is the direct transform of the finite data from the time to the frequency domain, it is the least squares representation of the raw data (convolved with a window), and it contains the raw coefficents of the Fourier line spectrum. For random signals, the individual component amplitudes do not converge to the true spectrum as the data record length increases. To estimate the true spectrum for the process, adjacent values of the line spectrum are summed together. If too many points are summed together the spectrum becomes oversmoothed (biased). The appropriate number of points to sum to best approximate the true spectrum is more of an art than a science. The window most commonly applied to the data for the FFT technique is the tapered cosine window where the first and last 10 percent of the time series is smoothed using a quarter period segment of the cosine function. The effect of varying the number of line spectral components summed together will be considered further.

The lag product method involves transforming a number of lags of the autocovariance function. The resulting spectral estimate is a function of the number of lags transformed and the window used to multiply the autocovariance function (lag window). When the number of lags transformed is too few the spectrum is oversmoothed (biased). As the number of lags increases, the spectrum approaches the true spectrum of the autocovariance function, then becomes very jagged and unstable. The jagged spectrum produced by the lag product method does not converge to the raw line spectrum produced by the FFT technique. The number of lags necessary to produce the best estimate is unknown and will be considered further. Several window functions are commonly used to smooth the spectral estimate and minimize the effects of side loops (Jenkins and Watts, 1968).

A decision must be made about which combination of windows and transform techniques should be used to produce the best estimate of spectra for coexisting waves which can then be broken into frequency components and used as inputs into the decomposition technique. Experimental data were acquired at four stations simultaneously; two in front of a solid wall (7'9" and 12'9")

and two at the same distances in front of a perforated wall breakwater, 150 feet away (Figure 1). The co-existing waves at the two stations should be different because of the different reflecting processes, but the energy density of the incident waves averaged over the 5.6 minutes of the record should be the same at two stations only 150 feet apart. Decomposition can be used to compute the incident spectra and average energy density (proportional to the variance) at the two locations. A perfect estimate of the actual incident wave process would require that the incident variance at the two locations be identical. Defining this desired condition as C,

$$C = \sqrt{\frac{\sigma^2_{i_\infty}}{\sigma^2_{i_{BW}}}} \rightarrow 1 \qquad (9)$$

where a perfect decomposition requires C = 1.

Reflections from a solid vertical wall are nearly perfect below a critical wave camber (Morden, 1975, Section IIC). Over most of the wave conditions encountered in the present investigation, the reflection coefficient in front of the solid wall, R_∞, should equal .99-1.0. Co-existing wave data in front of the wall can be decomposed and the resulting variances for the incident and reflected components used to obtain R .

$$R_\infty = \sqrt{\frac{\sigma^2_{r_\infty}}{\sigma^2_{i_\infty}}} \rightarrow .99\text{-}1.0 \qquad (10)$$

A perfect decomposition requires R_∞ = .99-1.0.

Perforated walled breakwaters reduce co-existing wave action enough that several observers qualitatively claim that the devices work well. A reduction in co-existing waves substantial enough to be clearly seen in a random sea state would require a considerable dissipation during the reflection process. Therefore, properly decomposed spectra should show a reflection coefficient significantly less than 1. Model-scale predicitons (Richey and Sollitt, 1970) suggest overall reflection coefficient (R_{BW}) values in the range of 0.4 to 0.7.

$$R_{BW} = \sqrt{\frac{\sigma^2_{r_{BW}}}{\sigma^2_{i_{BW}}}} \rightarrow .4 \text{ to } .7 \qquad (11)$$

These criteria can now be applied to the data for various combinations of lags and windows for the lag product techniques and various sums of spectral line components for the FFT technique. The variations are applied to the co-existing wave data, the resulting spectra can then be incremented and used as inputs into the decomposition technique. The computed incident and reflected variances and spectra can then be judged by the natural criteria.

Stationarity was established for each set of data by analysing the different portions of long analog data records and using only those without changes in computed spectra. Following analysis of many combinations the data was digitized and sampled with a sampling rate of .328 second/sample. (Nyquist frequency 1.52 Hz) 1024 data points represent 5.6 minutes of analog data.

Jenkins' and Watts' (1968) window closing technique was initially used to examine 20, 40, 60, 80 and 95 lags of the co-existing wave data. The lag product method produces very smooth unbiased input spectra when the number of lags equals 50, approximately 5 percent of the record length. Progressive wave spectra often become unstable with lag numbers approaching twice this number. Since the co-existing wave record is expected to be much less smooth because of the effects of partial nodes and antinodes, a high number of lags, say 95, were also tried. The window which produces the least stable spectra is the rectangular window (with its large negative side loops). Tukey and Parzens windows were also applied to smooth the spectra (with the Parzens window presenting the advantage of no negative side loops). The effect of the extremes of these conditions on the shape of the co-existing wave data is shown in Morden (1975). The resulting incident and reflected spectra can be grouped to display the spectral shapes corresponding to the natural criteria. Even transforming 95 lags of the autocovariance of a co-existing sea state produces a spectrum (convolved with appropriate window) which is too smooth to be broken into increments which can be treated independently.

The FFT technique provides the advantage of transforming the data directly. The number of raw periodogram coefficients to be summed together to produce co-existing wave spectra can be varied to show their effect on the computed incident and reflected spectra. Sums of 3, 10, and 15 points (denoted $\sum 3$, $\sum 10$, $\sum 15$) were considered. To increase the number of line spectral components computed, zeroes can be added also to the record. The effect of adding the same number of zeroes as original data points was also considered. The tapered cosine window is an accepted window for use with FFT and is used in all the following comparisons (Bergland 1969). The FFT spectra appear less smooth than those computed from the lag product method, and they do satisfy all three criteria.

Table I summarizes the results of applying the various conditions above to the arbitrarily chosen data set. In all cases the reflection co-efficients are defined over the range of frequencies containing measurable data, .25 to .65 Hz. Application of FFT $\sum 3$ to fourteen sets of field data records produced root mean square error from the criteria for perfect estimation of 4.0 percent for the reflection coefficient (Eq. 10) and 12.7 percent for C (Eq. 9). FFT $\sum 10$ with zeroes added produced r.m.s. values of 3.9 percent for all R_∞ and 10.7 percent for all C.

It is concluded that the decomposition technique is indeed sensitive to the shape of the input co-existing wave spectra. The lag product method, with its intermediate computation and transformation of the autocovariance function, produces too much smoothing to allow independent treatment of frequency increments. While not perfect, the decomposition technique incorporating the FFT produced input spectra is capable of reducing co-existing wave spectra differing by almost an order of magnitude and produce spectra which satisfy the established criteria within 10 percent.

Based on the examination of the available data, the FFT technique incorporating the summation of 10 spectral line components of co-existing wave data with zeroes added is recommended. Finally, it is suggested that any desired smoothing be done on the output incident and reflected spectra after decomposition. One effective smoothing technique is the moving average.

TABLE I. SUMMARY OF TECHNIQUES APPLIED TO AN ARBITRARY DATA SET (DATA 16-156/157)

CO-EXISTING WAVE DATA - INPUT										
			SOLID WALL Sensor Data					BREAKWATER Sensor Data			
Technique	Lag or Sum	Window	σ^2 outer	fq	σ^2 inner	fq		σ^2outer	fq	σ^2inner	fq
LP	95	Rect.	.00549	.49	.00104	.53		.00347	.50	.00120	.46
LP	95	Parz.	.00549	.49	.00104	.52		.00347	.49	.00120	.46
LP	95	Tuk.	.00549	.49	.00104	.53		.00347	.50	.00120	.46
LP	50	Parz.	.00549	.49	.00104	.52		.00347	.49	.00120	.47
LP	50	Tuk.	.00549	.49	.00104	.52		.00347	.49	.00120	.46
FFT	∑3	T.C.	.00568	.50	.00101	.50		.00385	.50	.00130	.50
FFT	∑10	T.C.	.00568	.49	.00117	.55		.00385	.49	.00130	.46
FFT (w/z)	∑10	T.C.	.00568	.48	.00112	.52		.00371	.48	.00128	.45
FFT (w/z)	∑15	T.C.	.00568	.48	.00112	.55		.00370	.52	.00113	.46

OUTPUT FROM DECOMPOSITION TECHNIQUE													
			SOLID WALL					BREAKWATER					
			Reflected		Incident			Reflected		Incident			
Technique	Lag or Sum	Window	σ_r^2	fq	σ_i^2	fq	R_∞	σ_r^2	fq	σ_i^2	fq	R_{BW}	C
LP	95	Rect.	.00178	.49	.00172	.47	1.01	.00134	.46	.00160	.50	.92	1.04
LP	95	Parz.	.00161	.49	.00173	.47	.96	.00132	.48	.00165	.50	.89	1.03
LP	95	Tuk.	.00166	.49	.00176	.47	.97	.00131	.49	.00163	.50	.90	1.04
LP	50	Parz.	.00160	.49	.00168	.47	.98	.00136	.46	.00168	.50	.90	1.00
LP	50	Tuk.	.00159	.49	.00172	.49	.96	.00133	.46	.00166	.49	.89	1.02
FFT	∑3	T.C.	.00180	.50	.00179	.50	1.00	.00066	.50	.00183	.49	.60	.99
FFT	∑10	T.C.	.00183	.50	.00182	.47	1.00	.00060	.49	.00188	.49	.56	.98
FFT (w/z)	∑10	T.C.	.00175	.48	.00179	.47	.99	.00062	.50	.00179	.50	.59	1.00
FFT	∑15	T.C.	.00175	.48	.00175	.46	1.00	.00057	.50	.00178	.50	.57	.99

LP = Lag Product Method

FFT = Fast Fourier Technique

(w/z) = with zeroes added

σ^2outer = Variance at outer gage

σ^2inner = Variance at inner gage

σ_r^2 = Calculated variance for reflected wave system

σ_i^2 = Calculated variance for incident wave system

fq = Frequency of peak spectral ordinate

Since the variance is not affected, the application of smoothing to the final computed incident and reflected spectra would primarily be for visual effect. (This was not done on any spectra shown.) Comparison of smoothed spectra could affect the incremental reflection coefficients, but not the overall reflection coefficient.

CONCLUSIONS AND RECOMMENDATIONS

Sea states where wind-generated waves and their reflections co-exist cannot be analyzed using the techniques commonly applied to progressive random waves. The co-existing sea surface consists of modulated waves contained in a complicated standing wave envelope. As a consequence, the time-averaged energy density varies continuously with position along wave rays. The average energy in a co-existing wave at any fixed location was shown to be a function of a phase relationship as well as the incident and reflected wave amplitudes.

By combining the appropriate spectral analysis with a theory based on linear waves relationships, the stochastic process of wind generated waves and their reflection are amenable to analysis in spite of their deterministic phase relationships. The decomposition technique provides a means of separating incident and reflected wave spectra using spectral estimates computed from data obtained simultaneously at two fixed, in-line sensor locations in wave fields where incident and reflected waves co-exist. Data from either surface or sub-surface sensors can be used, provided the wave energy is sufficiently narrow banded to allow filtering of the "twice frequency hump." The distance, x_2, between sensors affects the maximum frequency component obtainable in the decomposed spectra. ($f_{max} = \sqrt{x_2/2.56}$ for deep water waves). Though it is necessary to know or assume that the frequency of a wave component is unaltered during the reflection process, no other knowledge is needed of either the location or fluid dynamics of the reflection.

The accuracy of the technique depends on the spectral analysis method applied to estimate the co-existing wave spectrum. The fast Fourier transform method, which produces a spectrum by directly transforming the digitized data, provides a more accurate assessment of reflection characteristics than the lag product or autocovariance method. Based on the application of validation criteria to field test data obtained in wind generated deep water waves, it is recommended that a number of zeroes equal to the length of the digital data record be added to the co-existing wave data before analysis, that the tapered cosine window be applied, and that ten components of raw periodogram be summed together to produce the best input spectra for the decomposition technique.

As a result of accurate decomposition, the characteristics of waves reflected from, and the dissipation of wave energy occurring at, a barrier can be quantitatively evaluated for any reflected wave process where the wave frequency is not significantly altered during reflection.

REFERENCES

Morden, Dennis B., "The Decomposition of Co-existing Random Incident and Reflected Wave Energy," Ph. D. Dissertation, University of Washington, 1975.

Richey, E. P. and C. K. Sollitt, "Wave Attenuation by Porous Walled Breakwater," Journal of Waterways, Harbors and Coastal Engineering Division, ASCE, 69, WW3, New York, New York, August 1970, p. 643-663.

Ippen, A. T., ed., Estuary and Coastline Hydrodynamics, Engineering Societies Monographs, McGraw-Hill Book Co., 1966.

Thornton, E. B. and R. J. Calhoun, "Spectral Resolution of Breakwater Reflected Waves," Journal of Waterways, Harbors, and Coastal Engineering Division, ASCE, 98, November, 1972, p. 443-460.

Brigham, E. L., The Fast Fourier Transform, Prentice Hall, Inc., Englewood Cliffs, New Jersey, 1974.

Bergland, G. E., "A Guided Tour of the Fast Fourier Transform," IEEE Spectrum, 6, July 1969, p. 41-52.

Paniker, N. N., "Determination of Directional Spectra of Ocean Waves from Gage Arrays," University of California Hydraulic Engineering Laboratory Research Report HEL 1-18, August, 1971.

Jenkins, G. M. and D. G. Watts, Spectral Analysis and Its Applications, Holden-Day, INc., San Francisco, 1968.